Full Paper Wiley Online Library ELECTROANALYSIS

DOI: 10.1002/elan.201500375

# Enhanced Hydrogen Peroxide Sensing Based on Tetraruthenated Porphyrins/Nafion/Glassy Carbon-modified Electrodes via Incorporating of Carbon Nanotubes

Karla Calfumán,*[a] Diego Quezada,[b] Mauricio Isaacs,[b] and Soledad Bollo[c]

**Abstract**: The incorporation of carbon nanotubes to a Nafion/tetraruthenated cobalt porphyrin/ glassy carbon electrode (GC/Nf/CoTRP vs GC/Nf/CNTCoTRP) enhanced the amperometric determination of hydrogen peroxide. Both electrodes produced a decrease in the overpotential required for the hydrogen peroxide oxidation in about 100 mV compared to glassy carbon under the same experimental conditions. Nevertheless, for GC/Nf/CNT/CoTRP, the increase in the current is remarkable. The GC/Nf/CoTRP modified electrode gave no significant analitycal signal for hydrogen peroxide reduction. Moreover, a great increase in current is observed with GC/Nf/CNT/CoTRP at −150mV which suggests a significant increase in the sensitivity of the modified electrode. Scanning electrochemical microscopy (SECM) revealed an enhancement in the electroactivity of the GC/Nf/CNT/CoTRP modified electrode. This fact has been explained in terms of enhanced homogeneity of the electrodic surface as a consecuence of better dispersibility of CNT-CoTRP produced by a Nafion polyelectrolyte.

**Keywords:** Tetraruthenated porphyrins · Modified electrodes · Electrocatalysis · Nafion · Hydrogen peroxide · Carbon nanotubes

## 1 Introduction

Hydrogen peroxide can be found in a large number of commercial products and this fact has led to the development of several analytical methods for its quantification in many different areas of application, such as medicine, food, atmospheric and biochemical process [1]. For these reasons, various methods have been used to determine hydrogen peroxide, including the following: spectrophotometric [2,3], fluorimetric [4,5], chemiluminescence [6,7], chromatographic [8,9], volumetric [10,11] and electrochemical methods [1,12–17]. Electrochemical approaches are favorable for this determination due to the rapid response and simple operation.

Due to the high overvoltage requirement a direct amperometric detection scheme for hydrogen peroxide does not seem feasible in a complex sample from either an environmental or a biological sample [18]. A good way to reduce them is through the use of electrodes modified with redox mediators to aid the charge transfer processes. Some studies have reported the use of hexacyanoferrate [16], Prussian blue [14,19,20], metallic oxides [8,21,22], perovskites [23], carbon nanotubes [17,24,25], porphyrins [2,12,26] and phthalocyanines [27,28,29]. These compounds have been used as electrocatalysts for analytical purposes [12–28] or mimicking the activity of peroxidase [29,30], exhibiting excellent electrocatalytic behavior with a wide linear range of response; high sensitivity and low detection limit [26–29].

Tetraruthenated porphyrins are novel macrocycles, which present numerous redox processes, specifically Ru(III)/Ru(II) redox couple present a four electron simultaneous voltammetric wave that can be used as a redox probe for different analytical applications.

This kind of porphyrins contain four units of $[Ru(bpy)_2Cl]^+$ (bpy = 2,2′ bypyridine) coordinated to pyridinic moiety of a meso-tetra(pyridil)porphyrin i.e. a (TRP) [31]. One disadvantage in the use of these kinds of porphyrins is related with its high positive charge (4+), as this feature makes them soluble in water, re-dissolving the macrocycle from the electrodic surface to the working solution [32]. The modification of electrodic surfaces with mixtures of Nafion and MTRPs has shown to enhance the stability and the electrocatalytic properties of these macrocycles toward several analytes such as sulfite and nitrite anion [12,33,34].

On the other hand, physical and chemical properties of carbon nanotubes (CNTs) make them a good nano-structured material for different applications in a wide range of technological fields including biology, chemistry, medicine, electronic, materials and engineering [17,25]. CNT represents a carbon material which is found in two types:

[a] K. Calfumán
Facultad de Ciencias, Departamento de Química,
Universidad de Chile
Las Palmeras #3425, Casilla 653, Ñuñoa, Santiago, Chile
*e-mail: karlacalfuman@gmail.com

[b] D. Quezada, M. Isaacs
Facultad de Química,
Departamento de Química, Inorgánica,
Pontificia, Universidad de Católica Chile, Santiago, Chile

[c] S. Bollo
Facultad de Ciencias Químicas y Farmacéuticas
Departamento de Química Farmacológica y Toxicológica,
Universidad de Chile, Santiago, Chile

  

single-wall carbon nanotubes (SWCNTs) that can be described as a graphene sheet rolled into a cylinder and multiwall carbon nanotubes (MWCNTs) composed of concentric graphene sheets, namely, CNT of different diameters within each other. SWCNTs have a typical diameter between 1.2–5 nm, while for MWCNTs this value is between 10 and 50 nm [17,35]. The MWCNT modified electrodes show better performance due to its structure that showed a higher active area, since, as previous research has shown, both tube ends and defects in the walls are electrochemically active sites [17,35,36]. Recently, composites of metal nanoparticles [25,30] and porphyrins [37,38] have been prepared with CNT showing enhanced sensitivity towards small molecules such hydrogen peroxide [25], glucose [30], halides [37], nitrite [15,38] and methanol [39]. On the other hand, this combined surface between a good electrocatalysts and CNT is a potential platform toward the design of biosensors since it is known that MTRP allows electron transfer to enzymes and CNTs are able to immobilize biomolecules because keep a big active area and biocompatibility, enhancing the analytical performance of this potential biosensor [40].

The aim of this paper is the study of glassy carbon modified electrodes with Nafion polyelectrolyte as a support, tetraruthenated metalloporphyrin (M = Co(II), Ni(II) and Zn(II)) and MWCNT as electrocatalysts toward the electrochemical detection of hydrogen peroxide in neutral media. The effect of incorporating carbon nanotubes in the modification protocol was evaluated in terms of the enhancement in the sensitivity of the resulting method.

These modified electrodes have been quantitatively evaluated for amperometric detection of hydrogen peroxide at more favorable overpotential than bare glassy carbon in neutral media.

The best response was obtained in the hydrogen peroxide electroreduction performed at −150 mV presenting a low detection limit of 27.9 μM. Among all, electrochemical methods using these modified electrodes are a simple and sensible way to quantify hydrogen peroxide.

## 2 Materials and Methods

### 2.1 Reagents

All chemical reagents were analytically graded. Sodium perchlorate, Nafion 117 and ferrocene methanol (FcOH) were purchased from Sigma-Aldrich. Multiwall carbon nanotubes 1–5 mm long and (30 ± 14) nm diameter were obtained from NanoLab (USA).

Methanol and hydrogen peroxide (30% V/V aqueous solution) were purchased from Merck.

The precursor complex cis dichloro (2,2′-bipyrydine) ruthenium (II) dihydrate was prepared following the procedure described in the literature [41]. The supramolecular complexes of Co(II), Ni(II) and Zn(II) μ-{*meso*-5,10,15,20-tetra(pyridyl)porphyrin}tetrakis{bis(bipyridine)(chloride) ruthenium(II)} $(PF_6)_4$ were prepared by the method described by Toma et al. [31,32,41]. The purity of these compounds was checked by optical absorption spectroscopy, elemental analysis and $^1$H-NMR.

### 2.2 Apparatus

Cyclic Voltammetry (CV), amperometry and scanning electrochemical microscopy (SECM) measurements were carried out with a CHI 900 setup (CH Instruments). Electrochemical measurements using a rotatory disk electrode (RDE) were carried out with a speed control unit BAS RDE-I and BAS CV-50W.

Working electrodes were glassy carbon discs purchased from CH Instrument (r = 1.5 mm), the auxiliary electrode was a Pt wire and reference electrode was Ag/AgCl both from CH Instruments. All potentials are referred to this reference electrode. For SECM measurements a carbon fiber electrode (r = 0.5 mm) homemade served as SECM tip while glassy carbon electrodes (r = 1.5 mm) from CH Instrument were used as SECM substrate. A magnetic stirrer provided the convective transport when necessary.

### 2.3 Preparation of Modified Glassy Carbon Electrode

After each experiment, the GC electrode was cleaned by polishing with 0.3 μm and 0.05 μm alumina slurries. The electrode was rinsed with double distilled, deionized water and rinsed in an ultrasonic bath for 30 s, to remove any remaining alumina and then rinsed again with abundant deionized water.

The procedure for the preparation of the modified electrodes (ME) is described briefly below.

*GC/Nf-modified electrode.* Five microliters of 1% Nafion solution diluted in methanol was placed on the surface of the GC electrode, and it was allowed to dry at room temperature (drop coating) [33,34].

*GC/Nf/MTRP-modified electrode.* The electrode GC/Nf was dipped into a 1 mM methanolic solution of the complex for 4 min (dip coating). The electrode was left to dry at room temperature [33,34].

*GC/Nf/CNT-modified electrode.* The electrode surface (GC/Nf) is modified with 5 μL of a dispersion prepared from 1 mg of short multiwall nanotubes in methanolic nafion solution by sonication for 20 min.

*GC/Nf/CNT/CoTRP-modified electrode.* The electrode surface (GC/Nf/CNT) is modified with 8 μL of a dispersion prepared from 1mg of short multiwall nanotubes and 5 mM of CoTRP in methanolic alcoholic nafion solution by sonication for 30 min.

### 2.4 SECM Experiments

The experiments were carried out in aqueous solutions 0.1 M $NaClO_4$ pH 6, using Ferrocenemethanol (FcOH) as redox mediator. The tip potential was held at 0.600 V to produce the oxidation of FcOH, while the substrate potential was held at −0.100 V to permit the feedback be-

  

tween the electrodes, since FcOHox generated at the tip is reduced at this potential regenerating the parent FcOH.

Part of the film (no more than 1/3 of the surface) was removed from the glassy carbon modified electrode. Then, an approach curve was conducted on the bare glassy carbon surface at a tip scan rate of 0.5 μm s$^{-1}$. The tip was stopped when $i_T$ reached 1.25 times the value of $i_{T,\infty}$ ($i_{T,\infty}=4nFDCa$, where $F$ is the Faraday constant, $n$ is the number of electrons transferred in the tip reaction, $D$ is the diffusion coefficient of electroactive species, $C$ is the bulk concentration of the species and "$a$" is the tip radius). According to the theoretical curve that describes the dependence of the $i_T$ with the distance between the tip and the substrate ($d$), 1.25 times of $i_{T,\infty}$ corresponds to a $d=\sim$10 μm, when a 5 μm tip radius is used [42].

After the approach curve, the tip was moved in the $x$-direction to make sure that the tip is over the film and a series of constant height 100 μm × 100 μm areas SECM images were recorded at a tip scan rate of 1 μm s$^{-1}$. The results are presented in the dimensionless form of $I_T$, by normalizing the experimental feedback current ($i_T$) by the steady-state current obtained when the tip was far from the substrate ($i_{T,\infty}$), i.e., $I_T=i_T/i_{T,\infty}$.

### 2.5 Cyclic Voltammetry and Amperommetry Measurements

The cyclic voltammetry and amperometry experiments were performed using a 0.10 M $NaClO_4$ (pH 6) as supporting electrolyte. All the experiments were carried out at room temperature.

## 3 Results and Discussion

### 3.1 Hydrodynamic Study of the Hydrogen Peroxide at the GC/Nf/MTRP Modified Electrodes

Figure 1 shows the current-potential performance generated from hydrodynamic voltammograms for GC, GC/Nf/CoTRP, GC/Nf/NiTRP and GC/Nf/ZnTRP modified electrodes, in order to evaluate the effect of the metal ion center present in the porphyrin ring, in presence of 0.01 M $H_2O_2$ and 0.1 M $NaClO_4$ as supporting electrolyte.

Figure 1 shows that the modified electrodes decrease the overpotential required for the hydrogen peroxide oxidation in about 100 mV, compared to glassy carbon, and an increase in the associated currents that clearly indicates the catalytic activity of MTRP towards oxidation of hydrogen peroxide. This effect is more pronounced at the electrode containing CoTRP.

Also the formation of a molecular stacking of tetraruthenated porphyrins on nafion polymer matrix and/or electrode surface has been reported [12,43,44].

Acording to Da Rocha et al. [43] charge transfer mechanism in molecular stacks are based in four key points detailed below.

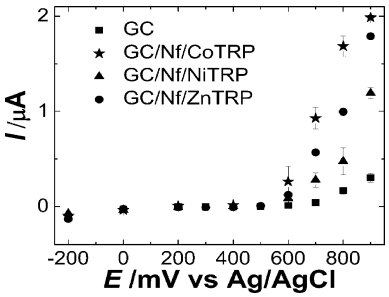


Fig. 1. Steady-state current versus applied potential of GC (■), GC/Nf/CoTRP (★), GC/Nf/NiTRP (▲) and GC/Nf/ZnTRP (●) obtained for the electrochemical reduction of $H_2O_2$ (0.01 M) in $NaClO_4$ (0.1 M) aqueous solution.

i. Hole generation from the electrode to the ruthenium complexes disposed next to the electrodic surface and its propagation trough the porphyrin π system.
ii. Hole generation by jump of electrons only involving the peripheral ruthenium complexes.
iii. Hole generation by jump of electrons involving the metal ion coordinated to the porphyrin core.
iv. Through pure electronic conduction across the porphyrin π system.

Therefore, according to the available information and considering that all the charge transfer mechanism above mentioned occurs, it is possible to suppose that the difference in catalytic activity toward hydrogen peroxide shown by the different modified electrodes should be directly related to the formation of porphyrin molecular stacks on the nafion polymeric matrix and/or on the electrode.

Considering that molecular stacks will depend of the stacking capacity, an intrinsic characteristic of each macrocycle, the formation of molecular stacks will depend directly on the number of electrons in the d orbitals of metal center coordinated to the porphyrin; hence, promoting or preventing charge transfer according to the above mentioned mechanism *iii*.

Among the metals studied, Ni(II) is the only one that can maintain the symmetry plane when it is coordinated in the center of the macrocycle, fact which agrees with the lower catalytic activity. On the other hand, Co(II) and Zn(II) present larger ionic radius, therefore, when inserted in the central cavity, a change in the porphyrin symetry is expected, mainly due to its position out of the macrocycle plane. Due to this reason, molecular stacking capacity should be increased because of their random stacking, making a faster charge transfer through the polymeric matrix. In addition it must be considered that Co(II) in a square planar geometry afford a free molecular orbital able to bind oxo-species like $O_2$ and $H_2O_2$ previous to electron transfer [45]. In contrast a Zn(II) metal center is a closed shell ion without possibility of coordination of ligands (analytes) as a previous path to the electron transfer reaction. In consequence the enhanced molecular stacking ability of CoTRP and coordination prop-

  

erties of Co(II) ion as a metal center it must provide a synergism toward oxidation and reduction of $H_2O_2$ better than other metal ions studied in this work.

As CoTRP was the macrocycle that presents the best electrocatalytic activity, this complex was selected to evaluate the effect of incorporate CNTs in the electrodic surface.

### 3.2 Voltammetric Characterization of Modified Electrodes in $H_2O_2$ Electrocatalysis

The cyclic voltammetry of GC, GC/NTC, GC/Nf/CoTRP y GC/Nf/NTC/CoTRP modified electrodes in the oxidation of $H_2O_2$ is shown in Figure 2.

As shown in Figure 2 (C,D) $H_2O_2$ oxidation current on modified electrodes is several times higher than those registered for GC and GC/NTC (Figure 2A,B), confirming the electrocaytalytic character of these modified electrodes where the redox couple responsible for this process is Ru(III)/Ru(II) (see Figure 2C dotted line). Comparing both modified electrodes it is clear that GC/Nf/CoTRP presents a reversible character for $H_2O_2$ oxidation wheras in GC/Nf/CNT/CoTRP the oxidation of $H_2O_2$ occurs as a irreversible process (Figure 2C,D), also a significant enhanced in the oxidation current for $H_2O_2$ is observed in GC/Nf/CNT/CoTRP, these differences could be attributed to the incorporation of CNT to the mixture of the electrode, since CNT increase active of the electrode and enhance conducting proprteries of the surface [36,46].

The same experiments were carried for the reduction of $H_2O_2$ (not shown), again modified electrodes showed a better activity for the reaction under survey. In this case it has been informed that metal ion in the cavity of the macrocycle or a macrocycle reduction process it should be the active redox center. This fact has been demonstrated for $O_2$ and $CO_2$ reduction [45].

Figure 3 shows the current-potential plot taken from voltammograms under constant stirring for GC, GC/Nf/CoTRP and GC/CNT/Nf/CoTRP modified electrodes.

This figure shows the presence of CNT significantly improves the hydrogen peroxide electrooxidation and reduction ensuring a reliable electroanalytical quantification.

Incorporation of less than 5% w/w of carbon nanotubes has improved many properties in polymers, such as mechanic resistance, resistance to thermic degradation or thermal and electrical conductivity. However, increase of the aforementioned properties in a polymeric nanocompound requires the optimization of two conditions; the first one related to the CNT dispersion and secondly its integration to the polymeric matrix. In this study, an optimal dispertion has been reached, increasing the above mentioned properties in the GC/Nf/CoTRP modified electrode.

Thus based in cyclic and hydrodynamic voltammetry experiments (Figs. 1, 2 and 3), electroanalytical working potentials were chosen as the minimal necessary to carry out the reaction.

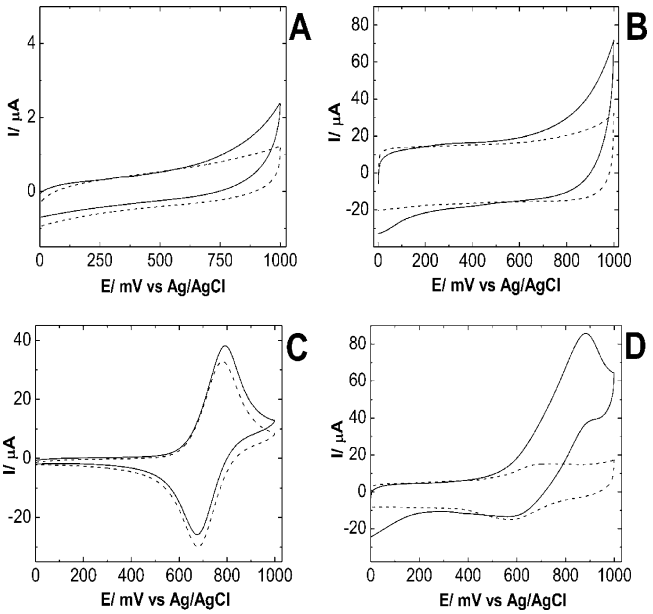


Fig. 2. Cyclic Voltammetry of A) GC, B) GC/CNT, C) GC/Nf/CoTRP and D) GC/Nf/CNT/CoTRP in ausence (dotted line) and presence (solid line) of 0.02 M $H_2O_2$ in 0.1 M $NaClO_4$ solution. Scan rate 100 mV/s.

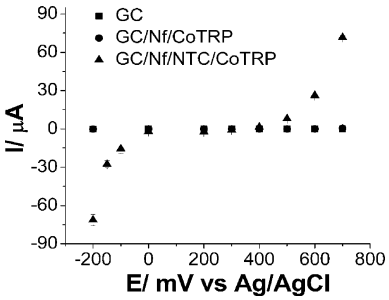


Fig. 3. Voltammetric behavior under constant stirring at GC, GC/Nf/CoTRP and GC/Nf/CNT/CoTRP modified electrodes in presence of 0.01 M $H_2O_2$ in 0.1 M $NaClO_4$.

### 3.3 Amperometric Oxidation of Hydrogen Peroxide at the GC/Nf/CNT/CoTRP Modified Electrodes

Since amperometry under constant stirring conditions is much more current sensitive than cyclic voltammetry, this method was employed in order to estimate the sensitivity of the electrodes to detect $H_2O_2$. Figure 4 depicts the corresponding calibration plots and amperometric experiments recorded at 600 mV obtained after sequential additions of hydrogen peroxide at GC/Nf/CNT/CoTRP modified electrode. These are shown in the insets of Figure 4.

In the above mentioned figure, a linear relationship between current response and the hydrogen peroxide concentration in the range 0 to 1 mM can be seen, while for a higher concentration of $H_2O_2$, the plot current versus analyte concentration deviates from linearity as a manifest of surface saturation.

  

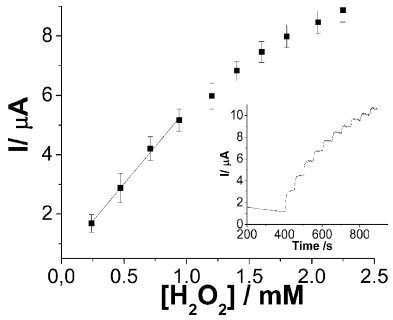


Fig. 4. Calibration curve. Inset: amperometric response of GC/Nf/CNT/CoTRP obtained at 600 mV for the modified electrode after successive additions of $H_2O_2$ 0.01 M in $NaClO_4$ 0.1 M.

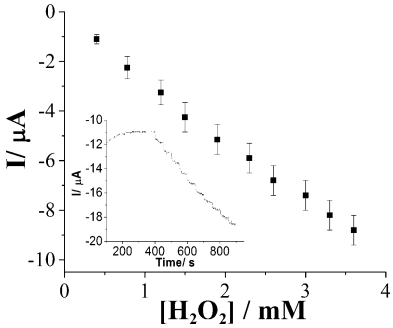


Fig. 5. Amperometric response of GC/Nf/CNT/CoTRP obtained at −150 mV for the modified electrode after successive additions of $H_2O_2$ 0.01 M in $NaClO_4$ 0.1 M.

The sensitivity of the sensors was estimated from the slopes of the linear concentration range and the value is 8 nA/μM (Table 1). The limits of detection (LODs) calculated as three times the standard deviation of the blank over the sensitivity was in the order of $10^{-6}$ M (Table 1). All the plots have linear coefficients above 0.99.

### 3.4 Amperometric reduction of Hydrogen Peroxide at the GC/Nf/CNT/CoTRP Modified Electrodes

Figure 5 depicts the corresponding calibration plots and amperometric experiments recorded at −150 mV obtained after sequential additions of hydrogen peroxide at GC/Nf/CNT/CoTRP modified electrode are shown in the insets of Figure 5.

There is a linear relation between the current response and peroxide concentration in the range 0 to 2.6 mM (Figure 5). The sensitivity of the sensors was estimated from the slopes of the linear concentration range and the value is 4.3 nA/μM (Table 1). The limits of detection (LODs) calculated as three times the standard deviation of the blank over the sensitivity was in the order of $10^{-6}$ M (Table 1). All the plots have linear coefficients above 0.99.

In a general GC/Nf/CNT/CoTRP presents a LOD in the same order of magnitude that several devices already published, but it must be considered that the overpotential for oxidation-reduction of $H_2O_2$ on GC/Nf/CNT/CoTRP modified electrode is significatively low. Comparing the results of the present work with other modified electrodes, see Table 1, it is observed that at oxidation potentials GC/Nf/CNT/CoTRP presents a lower limit of detection compared to a Nafion/PtPd-MWCNTs/GCE at the same operative potential. At reduction potentials GC/Nf/CNT/CoTRP presents lower LOD's that TH/DNA/nano-$TiO_2$/GC at very near workin potential. [13–16,43].

Table 1. Electroanalytic parameters for the determination of $H_2O_2$ at GC/Nf/CNT/CoTRP modified electrodes in 0.1 $NaClO_4$.

| Electrode $\mu M^{-1}$ | $E_{APPLIED}$/ mV | LOD/ μM | Sensitivity/ nA |
|---|---|---|---|
| GC/Nf/CNT/CoTRP | −150 | 27.9 | 4.3 |
| | 600 | 10.9 | 8.0 |
| AgPs-SWCNT[13] | −300 | 2.8 | – |
| AgNPs/PoPD/GCE[13] | −500 | 1.5 | – |
| Ag/GC electrode[13] | −440 | 10 | – |
| PQ11-AgNPs/GCE[13] | −300 | 33.9 | – |
| Ag/GN-R/GCE[13] | −400 | 28 | – |
| Nafion/PtPd-MWCNTs/GCE[13] | 600 | 31 | – |
| TH/DNA/nano-$TiO_2$/GC[16] | −200 | 50 | 6.1 |
| PdNPs[44] | −500 | 2 | 2.7 |

The modified electrodes can easily be regenerated by washing the surface with water; its catalytic activity remains almost unchanged. The results obtained for GC/Nf/CNT/CoTRP among them; the quick and easy preparation of modified electrode, production low cost in addition to its excellent stability and catalytic effect, show that this modified electrode can potentially be used for the determination and monitoring of $H_2O_2$.

### 3.5 Characterization of Modified Electrodes by Electrochemical Scanning Microscopy

In order to understand the topography and the electrochemical activity of the electrodic surfaces, SECM experiments were carried out [47,48]. Figure 6 shows the 3D SECM surface-plot images of the GC/Nf/CoTRP, GC/Nf/CNT/CoTRP and GC/Nf/CNT modified electrodes.

The electrode surface GC/Nf reveals an irregular electrochemical activity; this fact can be explained in terms of pores that are present in the polyelectrolyte film [33]. Thus, the generation of $FcOH_{ox}$ positively charged could be adsorbed in the negative pores of Nafion, covering the surface area and preventing any other charge transfer in this zone (not shown) [12,36]. In contrast, GC/Nf/CoTRP has a homogeneous electrochemical activity, normalized current presents values without variations, confirming the close interaction between polyelectrolyte and the macrocycles forming a layer of sufficient thickness to cover the polyelectrolyte surface entirely [12,49].

On the other hand, the ability of Nafion to disperse CNT provides a useful avenue for preparing CNT-based electrode transducers for a wide range of sensing applications [36]. Under the experimental conditions studied,

  

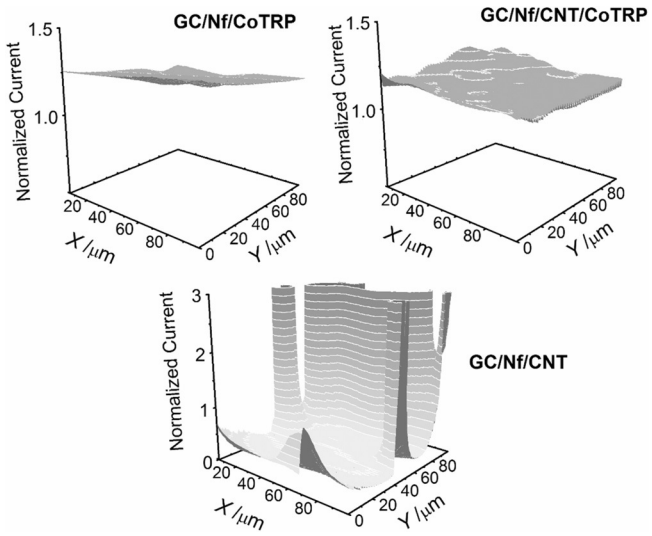


Fig. 6. 3D SECM surface-plot images of the modified electrode.

GC/Nf/NTC modified electrodes presenting clear evidence of enhanced surface activity compared with GC/Nf. However, the image shows regions with different electroactivity, suggesting the existence of areas with different amount of CNT indicating that the nanotubes are arranged randomly and not necessarily spatially ordered which could reduce their catalytic efficiency.

When CNT are dispersed in the presence of Nafion and CoTRP, the electrodic surface GC/Nf/CNT/CoTRP shows a homogeneous electrochemical activity indicating that specific interactions between CNT and CoTRP are favoring the CNT dispersability.

By comparing GC/Nf/CoTRP with GC/Nf/CNT/CoTRP, although both have similar catalytic activities (current values) and the electrode surface exhibit a comparable homogeneity, it may be noted that the CNT-modified electrode roughness is slightly higher; the result was clearly influenced by the CNTs.

The addition of CNTs contributing to the formation of a new molecular stacking different from that of MTRP by altering the shape, surface-morphology, composition chemical and physical properties including the catalytic activity. This new hybrid assemblies between CNT and MTRP by noncovalent π-π stacking, provides an excellent opportunity collectively combine the exceptional properties of these two materials [50]. In addition the use of CNT provide the ability to anchor biomolecules, thus projecting the use of this surface as a biosensor.

## 4 Conclusions

A simple procedure was used to modify glassy carbon electrodes using a tetraruthenated metalloporphyrin (M = Co (II), Ni (II) and Zn (II)) and Nafion polyelectrolyte as a support (GC/Nf/MTRP). These modified electrodes were compared with an analog that contained multiwall nanotubes (GC/Nf/CNT/CoTRP) in the amperometric oxidation and reduction of hydrogen peroxide in neutral media (0.1 M $NaClO_4$).

The GC/Nf/CNT/CoTRP modified electrode shows decrease of the potential required for the hydrogen peroxide reduction at about 150 mV compared to glassy carbon under the same experimental conditions and also presents low detection limit, high sensitivity, short response time, satisfactory linear concentration range excellent stability and good reproducibility.

Based on SECM experiments it was demonstrated that the CNTs provide increased roughness and therefore an enhanced active area.

## Acknowledgements

K. C. is grateful to CONICYT scholarships for PhD studies in Chile. K. C. acknowledges PhD scholarship support AT 24091042 and PhD exchange student program (BECAS CHILE); D. Q. thanks to CONICYT PhD scholarship 21120676. This work was supported by Proyect RC 130006 CILIS granted by Fondo de Innovacion para la Competitividad del Ministerio de Economia, Fomento y Turismo, Chile and Fondecyt Grant 1141199 and 1120246.

## References

[1] M. S. M. Quintino, H. Winnischofer, K. Araki, H. E. Toma, L. Agnes, *Analyst* **2005**, *130*, 221–226.
[2] A. C. Pappas, C. D. Stalikas, Y. C. Fiamegos, M. I. Karayannis, *Anal. Chim. Acta* **2002**, *455*, 305–313.
[3] L. D. Vieira, *Analyst* **1998**, *123*, 1809–1812.
[4] T. R. Holm, G. K. George, M. J. Barcelona, *Anal. Chem.* **1987**, *59*, 582–586.
[5] A. Sakuragawa, T. Taniai, T. Okutani, *Anal. Chim. Acta* **1998**, *374*, 191–200.
[6] N. Kiba, T. Tokizawa, S. Kato, M. Tachibana, K. Tani, H. Koizumi, M. Edo, E. Yonezawa, *Anal. Sci.* **2003**, *19*, 823–827.
[7] W. Qin, Z. Zhang, B. Li, S. Liu, *Anal. Chim. Acta* **1998**, *372*, 357–363.
[8] U. Pinkernell, S. Effkemann, U. Karst, *Anal. Chem.* **1997**, *69*, 3623–3627.
[9] J. Hong, J. Maguhn, D. Freitag, A. Kettrup, *J. Anal. Chem.* **1998**, *361*, 124–128.
[10] Y. T. Didenko, S. P. Pugach, *J. Phys. Chem. A* **1994**, *98*, 9742–9749.
[11] N. V. Klassen, D. Marchington, H. C. E. McGovan, *Anal. Chem.* **1994**, *66*, 2921–2925.
[12] K. Calfumán, M. J. Aguirre, P. Cañete-Rosales, S. Bollo, R. Llusar, M. Isaacs, *Electrochim. Acta* **2011**, *56*, 8484–8491.
[13] S. Chen, R. Yuan, Y. Chai, F. Hu, *Microchim. Acta* **2013**, *180*, 15–32.
[14] A. V. MoKrushina, M. Heim, E. E. Karyakina, A. Kuhn, A. A. Karyakin, *Electrochem. Comm.* **2013**, *29*, 78–80.
[15] V. Mani, B. Dinesh, S. M. Cheng, R. Saraswathi, *Biosensors and Biolectronics* **2014**, *53*, 420–427.
[16] A. Salimi, R. Rahmatpanah, R. Hallaj, M. Roushani, *Electrochim. Acta* **2013**, *95*, 60–70.
[17] K. González-Segura, P. Cañete-Rosales, R. Del Rio, C. Yañez, N. F. Ferreyra, G. A. Rivas, S. Bollo, *Electroanalysis* **2012**, *24*, 2317–2323.

  

[18] M. S. Lin, B. I. Jan, *Electroanal.* **1997**, *9*, 340–344.
[19] R. Araminaité, R. Garjonyté, A. Malinauskas, *J. Solid State Electrochem.* **2010**, *14*, 149–155.
[20] M. H. Pournaghi-Azar, F. Ahour, *J. Solid State Electrochem.* **2010**, *14*, 823–828.
[21] A. Salimi, R. Hallaj, S. Soltanian, H. Mamkhezri, *Anal. Chim. Acta* **2007**, *594*, 24–31.
[22] X. Bo, J. Bai, L. Wang, L. Guo, *Talanta* **2010**, *81*, 339–345.
[23] G. Luque, N. F. Ferreyra, A. G. Leyva, G. A. Rivas, *Sensor Actuators B–Chem.* **2009**, *142*, 331–336.
[24] Z. Li, X. Cui, J. Zheng, Q. Wang, Y. Lind, *Anal. Chim. Acta* **2007**, *597*, 238–244.
[25] C. Guzmán, G. Orozco, Y. Verde, S. Jiménez, L. A. Godínez, E. Juaristi, E. Bustos, *Electrochim. Acta* **2009**, *54*, 1728–1732.
[26] M. Shao, J. Han, W. Shi, M. Wei, X. Duan, *Electrochem. Commun.* **2010**, *12*, 1077–1080.
[27] K. I. Ozoemena, Z. Zhao, T. Nyokong, *Electrochem. Commun.* **2005**, *7*, 679–684.
[28] P. Mashazi, C. Togo, J. Limson, T. Nyokong, *J. Porphyrins Phtalocyanines* **2010**, *14*, 252–263.
[29] K. I. Ozoemena, T. Nyokong, *Electrochim. Acta* **2006**, *51*, 5131–5136.
[30] M. Shamsipur, M. Najafi, M. R. Milani, *Bioelectrochem.* **2010**, *77*, 120–124.
[31] K. Araki, H. Toma, *J. Coord. Chem.* **1993**, *30*, 9–17.
[32] K. Araki, H. Toma, *Coord. Chem. Rev.* **2000**, *196*, 307–329.
[33] K. Calfumán, M. J. Aguirre, D. Villagra, C. Yañez, C. Arévalo, B. Matsuhiro, L. Mendoza, M. Isaacs, *J. Solid State Electrochem.* **2010**, *14*, 1065–1072.
[34] K. Calfumán, M. García, M. J. Aguirre, B. Matzuhiro, L. Mendoza, M. Isaacs, *Electroanal.* **2010**, *22*, 338–344.
[35] J. Wang, *Electroanal.* **2005**, *17*, 7–17.
[36] M. Pumera, *Chem. Eur. J.* **2009**, *15*, 4970–4978.
[37] A. Salimi, H. MamKhezri, R. Hallaj, S. Zandi, *Electrochim. Acta* **2007**, *52*, 6097–6105.
[38] G. Turdean, I. C. Popescu, A. Curulli, G. Palleschi, *Electrochim. Acta* **2006**, *51*, 6435–6441.
[39] B. Sullivan, D. Salmon, T. Meyer, *Inorg. Chem.* **1978**, *17*, 3334–3341.
[40] Y. Wang, Z. Wang, Y. Rui, M. Li, *Biosensors and Bioelectronics* **2015**, *64*, 57–62.
[41] K. Araki, H. Toma, *J. Photochem. Photobiol.* **1994**, *83*, 245–250.
[42] A. J. Bard, M. V. Mirkin, *Scanning Electrochemical Microscopy*, in: M. Dekker (Ed.), New York, **2001**.
[43] J. C. Da Rocha, G. Dements, M. Bertotti, K. Araki, H. Toma, *J. Electroanal. Chem.* **2002**, *526*, 69–76.
[44] E. Trollund, P. Ardiles, M. J. Aguirre, S. R. Baggio, R. C. Rocha, *Polyhedron* **2000**, *19*, 2303–2312.
[45] E. Blair, F. Sulc, P. J. Farmer, *N-4 Macrociclyc metal complexes*, Ed. Springer, New York, **2006**.
[46] J. Wang, M. Musameh, Y. Lin, *J. Am. Chem. Soc.* **2003**, *125*, 2408–2409.
[47] P. Pang, Z. Yang, S. Xiao, J. Xie, Y Zhang, Y. Gao, *J. Electroanal. Chem.* **2014**, *737*, 27–33.
[48] A. J. Bard, F. R. F. Fan, J. Kwak, O. Lev, *Anal. Chem.* **1989**, *61*, 132–138.
[49] X. Lu, F. Zhi, H. Shang, X. Wang, Z. Xue, *Electrochim. Acta* **2010**, *55*, 3634–3642.
[50] C. Kung, P. Lin, F. J. Buse, Y. Xue, X. Yu, L. Dai, C. Liu, *Biosensors and Bioelectronics* **2014**, *52*, 1–7.

Received: June 22, 2015
Accepted: June 22, 2015
Published online: July 14, 2015

  